

Krylov complexity as an order parameter for quantum chaotic-integrable transitions

Matteo Baggioli,^{1,2,3} Kyoung-Bum Huh,^{1,2,3} Hyun-Sik Jeong,^{4,5} Keun-Young Kim^{6,7} and Juan F. Pedraza⁴

¹*School of Physics and Astronomy, Shanghai Jiao Tong University, Shanghai 200240, China*

²*Wilczek Quantum Center, School of Physics and Astronomy, Shanghai Jiao Tong University, Shanghai 200240, China*

³*Shanghai Research Center for Quantum Sciences, Shanghai 201315, China*

⁴*Instituto de Física Teórica UAM/CSIC, Calle Nicolás Cabrera 13-15, 28049 Madrid, Spain*

⁵*Departamento de Física Teórica, Universidad Autónoma de Madrid, Campus de Cantoblanco, 28049 Madrid, Spain*

⁶*Department of Physics and Photon Science, Gwangju Institute of Science and Technology, Gwangju 61005, Korea and*

⁷*Research Center for Photon Science Technology, Gwangju Institute of Science and Technology, Gwangju 61005, Korea*

Krylov complexity has recently emerged as a new paradigm to characterize quantum chaos in many-body systems. However, which features of Krylov complexity are prerogative of quantum chaotic systems and how they relate to more standard probes, such as spectral statistics or out-of-time-order correlators (OTOCs), remain open questions. Recent insights have revealed that in quantum chaotic systems Krylov state complexity exhibits a distinct peak during time evolution before settling into a well-understood late-time plateau. In this work, we propose that this Krylov complexity peak (KCP) is a hallmark of quantum chaotic systems and suggest that its height could serve as an ‘order parameter’ for quantum chaos. We demonstrate that the KCP effectively identifies chaotic-integrable transitions in the mass-deformed Sachdev-Ye-Kitaev model at both infinite and finite temperature, aligning with results from spectral statistics and OTOCs. Our findings offer a new diagnostic tool for quantum chaos that is operator-independent, potentially leading to more ‘universal’ insights and a deeper understanding of general properties in quantum chaotic systems.

Introduction. Chaos is a widespread phenomenon in nature. While substantial progress has been made in understanding classical chaos [1], its definition and characterization in the quantum realm, particularly in many-body systems, remain significantly less understood.

Traditionally, quantum chaos has been linked to the Bohigas-Giannoni-Schmit (BGS) conjecture [2–5], asserting that the energy spectra of quantum systems with chaotic classical counterparts match the statistical predictions of random matrix theory (RMT). Specifically, quantum chaotic systems are expected to display RMT features such as level repulsion and spectral rigidity [2, 6, 7], which are therefore accepted as fingerprints of late-time quantum chaos in many-body systems.

Conversely, in quantum chaotic systems at early times, the time evolution of specific out-of-time-order correlators (OTOCs) exhibits a phase of exponential growth [8, 9], governed by a non-zero Lyapunov exponent $\lambda_L \leq 2\pi k_B T/\hbar$ [10]. This behavior serves as an additional indicator of quantum chaos at complementary time scales.

Modern explorations of quantum chaos have prominently featured both level statistics and OTOCs, bolstered by intriguing links between many-body chaos and quantum gravitational systems [11–16]. In this context, Krylov complexity [17, 18] has recently emerged as a new valuable tool for characterizing quantum chaos, providing an alternative diagnostic beyond traditional analyses. It has been employed in RMT [18–22] and many other quantum chaotic systems, including quantum billiards [23–25], spin chains [26–31], and various flavors of the Sachdev–Ye–Kitaev (SYK) model [32–36]. Additionally, Krylov complexity has been discussed in several other contexts including topological and quantum phase

transitions [37–40], quantum batteries [41], bosonic systems describing ultra-cold atoms [42], saddle-dominated scrambling [43, 44], and open quantum systems [45–50] among others – see [51] for a comprehensive review. Two forms of Krylov complexity have been proposed in the literature: the original type, which addresses operator growth [17], and a newer version, which evaluates the spread of a time-evolving quantum state within a specific subspace of the Hilbert space [18]. The latter will be the focus of this Letter.

For time-evolved thermofield double (TFD) states in RMT (see [30] for a discussion on state-dependence of Krylov complexity), Krylov state complexity exhibits four distinct phases: an initial linear ramp, a peak, a subsequent decline, and a plateau. According to [18], the peak overshooting the plateau followed by a decline appears to be a universal characteristic of quantum chaotic many-body systems and is therefore expected to be absent in integrable systems.

Building on these observations, this Letter provides further evidence that the Krylov complexity peak (KCP) is a defining feature of quantum chaos, potentially serving as an ‘order parameter’ for quantum chaotic phases. Simply put, we propose that the KCP vanishes in integrable systems and that its height exhibits critical dynamics, capable of diagnosing quantum chaotic to integrable transitions at both infinite and finite temperature.

To provide evidence for our proposal, we turn to the SYK model and its variants, which serve as useful toy models. Specifically, we focus on the mass-deformed SYK model [52–54], which has been extensively studied for its relevance to quantum chaotic to integrable transitions, and has been thoroughly characterized through both level

statistics and properties of the OTOCs [54–60].

Deformed SYK model. We consider the mass-deformed SYK model [54], which involves N fermions in $0 + 1$ dimensions. This model extends the original SYK model [61] by including an additional quadratic term, known as the random mass term, alongside the random quartic interactions. The Hamiltonian of the model is

$$H = \frac{1}{4!} \sum_{i,j,k,l=1}^N J_{ijkl} \chi_i \chi_j \chi_k \chi_l + \frac{i}{2!} \sum_{i,j=1}^N \kappa_{ij} \chi_i \chi_j. \quad (1)$$

Here χ_i are Majorana fermions satisfying $\{\chi_i, \chi_j\} = \delta_{ij}$, residing in a Hilbert space of dimension $2^{\frac{N}{2}}$. The coupling constants J_{ijkl} and κ_{ij} are Gaussian-distributed random variables with zero mean. Their standard deviations are $\sqrt{6J/N^{3/2}}$ and κ/\sqrt{N} , respectively.

In the absence of a mass deformation, the SYK model is maximally chaotic and saturates the Maldacena-Shenker-Stanford bound on quantum chaos [10]. Conversely, the purely quadratic Hamiltonian corresponds to an integrable system, inherently lacking any chaotic hallmark. As the variance of the random mass deformation κ increases, the model transitions from chaotic to integrable, effectively detected through level statistics [54]. More precisely, the analysis of level spacing distribution and r -parameter statistics yield a critical value $\kappa_c \approx 66$ for $\beta = 0$. This transition is further confirmed by the out-of-time-ordered correlator (OTOC) and the value of the Lyapunov exponent, though there are open discussions on this point [57, 62]. Moreover, it has been analytically proven [63] that for $\kappa > \kappa_c$, all states are many-body localized, and spectral correlations are well described by Poisson statistics, as expected for an integrable system.

Overall, the deformed SYK model provides an ideal playground to test which features of Krylov complexity are unique to quantum chaotic systems and how they evolve as the system transitions to an integrable phase.

Krylov complexity and spectral form factor. The determination of Krylov complexity involves constructing the Krylov basis $\{|K_n\rangle\}$, achieved through the so-called Lanczos algorithm [64, 65]. This procedure yields two sets of Lanczos coefficients, $\{a_n, b_n\}$, that encapsulate all information regarding the dynamics of the state. These coefficients correspond to the tridiagonal elements of the Hamiltonian when expressed in the Krylov basis:

$$H|K_n\rangle = a_n|K_n\rangle + b_{n+1}|K_{n+1}\rangle + b_n|K_{n-1}\rangle. \quad (2)$$

Given the Lanczos coefficients, the Krylov wave functions $\psi_n(t)$ satisfy the iterative differential equation:

$$i \partial_t \psi_n(t) = a_n \psi_n(t) + b_{n+1} \psi_{n+1}(t) + b_n \psi_{n-1}(t), \quad (3)$$

which represents the Schrödinger equation within the Krylov space governed by the Hamiltonian H , such that the time-evolved state is given by $|\psi(t)\rangle = \sum_n \psi_n(t) |K_n\rangle$.

Finally, Krylov complexity is defined as

$$C(t) := \sum_n n |\psi_n(t)|^2. \quad (4)$$

It measures the average depth of a time-evolving state in the Krylov basis, reflecting the spread of the wave function in this basis.

As the initial state, we consider the TFD state,

$$|\psi(0)\rangle = \frac{1}{\sqrt{Z(\beta)}} \sum_n e^{-\frac{\beta E_n}{2}} |n\rangle \otimes |n\rangle, \quad (5)$$

where $Z(\beta) = \sum_n e^{-\beta E_n}$ is the partition function at inverse temperature β .

The spectral form factor (SFF) is another valuable tool to probe the dynamics of quantum chaos, which may be linked to level statistics. Specifically, for quantum systems with discrete energy levels $\{E_n\}$, the SFF is defined via the analytically continued partition function [4, 66],

$$\begin{aligned} \text{SFF}(t) &:= \frac{|Z(\beta + it)|^2}{|Z(\beta)|^2} \\ &= \frac{1}{Z(\beta)^2} \sum_{m,n} e^{-\beta(E_m + E_n)} e^{i(E_m - E_n)t}. \end{aligned} \quad (6)$$

Both in RMT and in the SYK model, $\text{SFF}(t)$ displays a characteristic slope-dip-ramp-plateau behavior.

Given the definitions provided in Eq.(4) and Eq.(6), it is natural to assume that a direct link between Krylov complexity and the SFF might exist. In fact, considering the Krylov complexity of the TFD state, the SFF can be interpreted as the survival probability of the time-evolved TFD state [21, 67]: $\text{SFF}(t) = |\psi_0(t)|^2$. Additionally, for the TFD state with $\beta = 0$, which is a maximally-entangled state, the late-time behavior of the Krylov complexity obeys the following identity [14, 32, 35, 68]

$$\lim_{T \rightarrow \infty} \frac{1}{T} \int_0^T \text{SFF}(t) dt = \frac{1}{1 + 2C(t \rightarrow \infty)}, \quad (7)$$

where $C(t \rightarrow \infty) = (d - 1)/2$, with d being the system size. This identity provides a non-local (in time) constraint relating $\text{SFF}(t)$ to $C(t)$, reminiscent of a sum rule.

Results. We calculate the time-dependent Krylov complexity, as defined in Eq.(4), for the mass-deformed SYK model as a function of the mass parameter κ and the inverse temperature β . We perform our computations with a system size of $N = 26$ and express all dimensionful quantities in units of the coupling J , following Ref.[54]. As noted in [18], $N = 26$ is sufficiently large to ensure convergence of the numerical results. Therefore, finite-size effects on Krylov complexity are minimal for this choice of N . For further details on the numerical methods, we refer the reader to the Supplemental Material.

In the top panel of Fig. 1, we show the normalized Krylov complexity $C(t)/d$ as a function of time for various values of $\kappa \in [0, 300]$, with colors ranging from **red** to **purple** at infinite temperature ($\beta = 0$). For low values of κ , Krylov complexity distinctly exhibits the four hallmark stages of chaotic dynamics: it first undergoes a linear ramp up to a peak at $t = t_{\text{peak}}$, followed by a decline that levels off into a constant plateau. The value

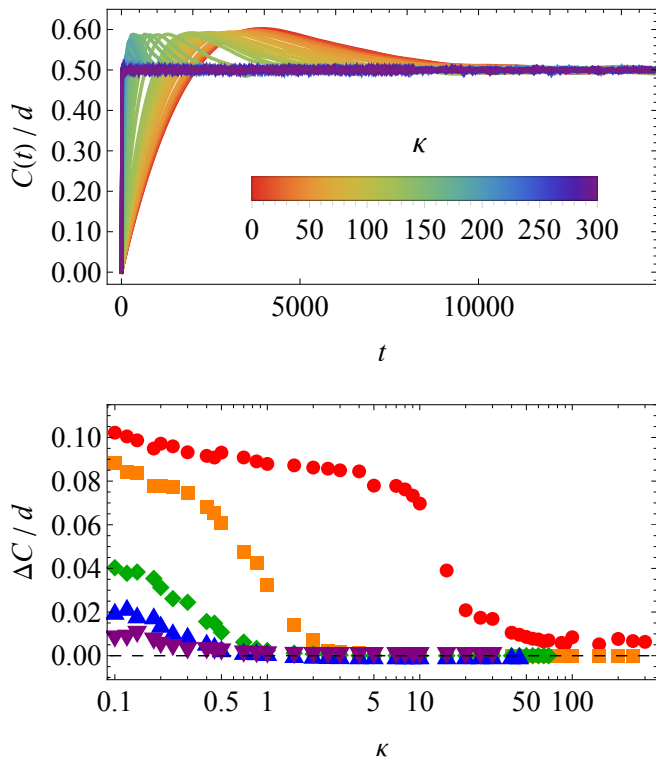


Figure 1. **Top:** Normalized Krylov complexity $C(t)/d$ with the TFD as initial state for various values of the parameter $\kappa = 0$ (red) to 300 (purple) for $N = 26$ and $\beta = 0$. **Bottom:** Normalized difference between the peak value $C(t = t_{\text{peak}})$ and the late time value $C(t \rightarrow \infty)$, as a function of κ for $\beta = 0, 1, 3, 5, 10$ (red, orange, green, blue, purple).

of $C(t)$ at the plateau as $t \rightarrow \infty$ is independent of the parameter κ , only depending on the system size, with $C(t \rightarrow \infty)/d \approx 1/2$. Furthermore, as κ increases, we note the KCP occurs at progressively earlier times and eventually vanishes when κ becomes sufficiently large.

These observations indicate that the peak in Krylov complexity could be used as a clear indicator for quantum chaos, disappearing when the system becomes integrable, *i.e.*, for large κ . To formalize this idea, we propose an ‘order parameter’ derived from the KCP. This parameter can be defined as the difference between the peak value $C(t = t_{\text{peak}})$ and the late time average (plateau) value $C(t \rightarrow \infty)$ of Krylov complexity,

$$\Delta C := C(t = t_{\text{peak}}) - C(t \rightarrow \infty). \quad (8)$$

By definition, $\Delta C \neq 0$ identifies a quantum chaotic system, while $\Delta C = 0$ indicates an integrable one.

In the bottom panel of Fig. 1, we present the KCP order parameter ΔC as a function of κ for various values of the inverse temperature β . The case at infinite temperature ($\beta = 0$), depicted in red, shows a smooth transition from $\Delta C \approx 0.1$ at $\kappa \rightarrow 0$ to a complete vanishing of ΔC at large κ . The critical value of κ at which this transition occurs aligns with the critical value $\kappa_c \approx 66$ reported in [54] based on spectral statistics methods.

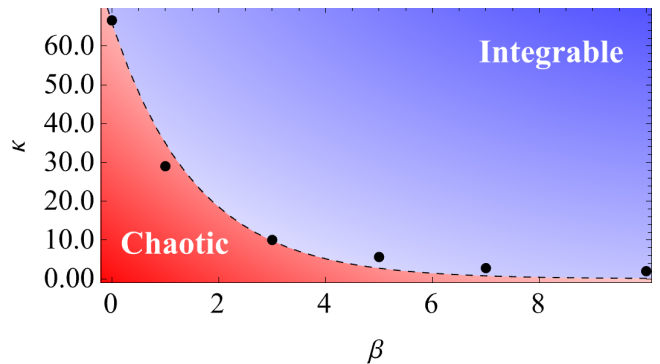


Figure 2. Phase diagram of the mass-deformed SYK model as a function of the parameter κ and the inverse temperature β . Black dots indicate the critical values of κ at which the KCP order parameter, as shown in Fig.1, vanishes. The dashed line represents the exponential fit given by Eq.(9). The lower region (red) denotes the chaotic phase, while the upper region (blue) represents the integrable phase, with the dashed line marking the boundary between these two phases.

As β increases and we move away from the infinite temperature limit, three key phenomena are observed. (I) In the quantum chaotic phase (small κ), the value of ΔC decreases, indicating that the height of the peak in $C(t)$ relative to the late-time plateau value becomes temperature-dependent. This behavior is consistent with the results for $\kappa = 0$ reported in [18]. (II) The point of continuous transition from $\Delta C \neq 0$ to $\Delta C = 0$ shifts to lower values of κ . (III) The width of this transition increases, with the KCP order parameter exhibiting a smooth crossover rather than a sharp critical transition.

We define the critical point by identifying the value κ_c at which the KCP order parameter vanishes, analogous to the vanishing of the Lyapunov exponent observed in the OTOC analysis of [54]. Using this definition, we construct a phase diagram for the mass-deformed SYK model as a function of the mass deformation parameter κ and the inverse temperature β . This phase diagram is illustrated in Fig. 2, with chaotic and integrable phases depicted in red and blue colors, respectively.

As the temperature decreases, the integrable phase becomes more favorable, and the critical point shifts to smaller values of κ . We observe that the critical line separating the chaotic and integrable phases is well described by an empirical exponential function:

$$\kappa_c(\beta) \approx \kappa_c(0) e^{-\frac{2}{\pi}\beta}, \quad (9)$$

which is shown as a black dashed line in Fig. 2. This indicates a strong dependence on the inverse temperature β . This behavior can be potentially rationalized by noting that higher temperatures enable the system to explore a broader range of energy states, leading to a more comprehensive representation of its spectral statistics. Additionally, the observed trend of the critical point with respect to β aligns well with previous results obtained using alternative methods [54].

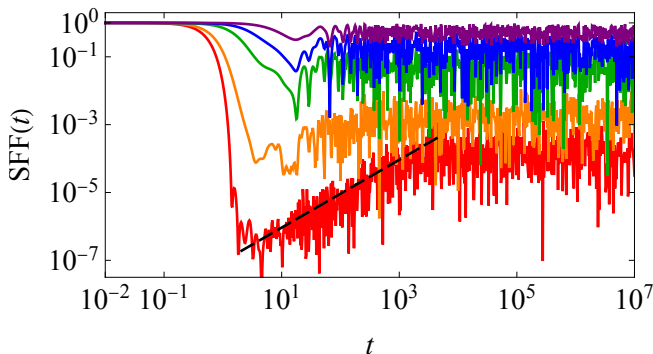


Figure 3. Spectral form factor, Eq. (6), as a function of time for $\kappa = 1$, $N = 26$ and $\beta = 0, 1, 3, 5, 10$ (red, orange, green, blue, purple). The black dashed line indicates the average linear growth characteristic of the SFF in the ramp regime.

Having established that the KCP is a signature of quantum chaotic states and a useful order parameter for detecting transitions from chaotic to integrable phases in many-body quantum systems, we now delve deeper into the relationship between Krylov complexity and the spectral form factor (SFF), as defined in Eq.(6). The mass-deformed SYK model is especially advantageous for this investigation, as it enables a comparative analysis both within the quantum chaotic regime and across the transition to its integrable phase.

A key feature of the SFF for chaotic systems is the presence of an extended linear ramp [4] that follows after the dip. In Fig. 3, we display the time-dependent SFF for various inverse temperatures β . For the quantum chaotic case with $\beta = 0$ (red), the linear ramp is clearly observed as indicated by the black dashed line in Fig. 3. Moreover, we have verified explicitly that the relation with the late time value of Krylov complexity, Eq. (7), is obeyed to a high degree of accuracy. As β increases, several notable changes occur. First, the $t \rightarrow \infty$ value of $SFF(t)$ rises, approaching the initial value of 1 as β becomes large. Second, the intermediate-time dip in $SFF(t)$ diminishes with increasing β and eventually disappears in the large β limit. Most significantly, the extent of the linear ramp decreases as β increases, ultimately vanishing as the inverse temperature approaches higher values.

Using the empirical function from Eq.(9) and taking $\kappa_c(0) \approx 66$, we estimate that for $\kappa = 1$, the critical value of β separating chaotic and integrable phases is approximately $\beta_c \approx 6.58$. This value lies in between the blue and purple lines in Fig. 3. Our numerical results show that this prediction, derived from the new KCP order parameter, matches the observed disappearance of the linear ramp in $SFF(t)$. This agreement not only verifies that the presence of a linear ramp and corresponding dip are clear indicators of quantum chaotic systems, which disappear as the system becomes integrable, but it also independently supports the validity and utility of the order parameter ΔC as a reliable benchmark for assessing quantum chaotic behavior.

These observations hint at a deeper relationship between Krylov complexity $C(t)$ and the SFF(t) that extends beyond the constraints described in Eq. (7). As noted in [69], a potential connection between the KCP and the linear ramp observed in the SFF seems to be emerging. Additionally, variations of the SFF explored in previous studies [54, 55] merit further investigation, particularly regarding their relation and potential interplay with Krylov complexity.

Discussion. In this Letter, we proposed that the KCP may serve as a defining feature of quantum chaos and could act as a robust ‘order parameter’ for identifying quantum chaotic phases in many-body systems. We observed that the KCP vanishes in integrable systems while displaying critical dynamics across chaotic-to-integrable quantum and thermal transitions. By computing the KCP using the TFD as an initial state, we effectively identified the chaotic-integrable transitions in the mass-deformed SYK model at both infinite and finite temperature. This finding is consistent with the results obtained from traditional probes such as spectral statistics and out-of-time-order correlators, and aligns with the independent prediction from the SFF.

Our results provide a compelling answer to the question of which features of Krylov complexity are unique to quantum chaotic systems and how these features change as the system transitions towards integrable regimes. It is now essential to further test our proposal and determine whether the KCP is a universal probe of quantum chaos, comparable to well-established concepts like level repulsion or the quantum Lyapunov exponent. In this vein, it is important to gain a deeper understanding of potential counterexamples, such as quantum systems with integrable phases exhibiting saddle-dominated scrambling, like the Lipkin-Meshkov-Glick model [43, 44], or quantum systems with a mixed phase space, such as the stringy matrix models recently considered in [70].

Lastly, our analysis underscores the unique importance of the TFD state in the study of quantum chaos in many-body systems, building on previous observations [30]. This state is crucial for Krylov complexity to effectively probe random matrix physics, likely because random matrix behavior encompasses the entire level-spacing spectrum of the system. Consequently, any measure aimed at probing random matrix behavior benefits from the TFD state’s ability to encompass the full spectrum. TFD states also play a significant role in holography, serving as CFT duals of two-sided black holes [71]. Recent findings suggest a connection between the Krylov complexity of chord states in the double-scaled SYK model and the length of the dual Lorentzian wormhole in Jackiw-Teitelboim gravity [72], a lower-dimensional realization of holography. Therefore, our work might provide valuable insights into the holographic dual description of chaotic-integrable transitions in quantum systems and contribute to addressing the profound and long-standing ‘million-dollar question’ of quantum gravity.

Note added: While this paper was in preparation, [22, 31, 36] appeared, partially overlapping with our scope.

ACKNOWLEDGMENTS

We would like to thank Antonio M. Garcia-Garcia for collaboration at the initial stage of this project and Junggi Yoon for valuable suggestions. We would like to thank Pratik Nandy and Debodirna Ghosh for useful comments on a first version of this manuscript. MB would also like to thank Dario Rosa for illuminating discussions on complexity and quantum chaos. MB and KBH acknowledge the support of the Shanghai Municipal Science and Technology Major Project (Grant No.2019SHZDZX01). M.B. acknowledges the sponsorship from the Yangyang Development Fund. HSJ and JFP are supported by the Spanish MINECO

‘Centro de Excelencia Severo Ochoa’ program under grant SEV-2012-0249, the Comunidad de Madrid ‘Atracción de Talento’ program (ATCAM) grant 2020-T1/TIC-20495, the Spanish Research Agency via grants CEX2020-001007-S and PID2021-123017NB-I00, funded by MCIN/AEI/10.13039/501100011033, and ERDF A way of making Europe. KYK was supported by the Basic Science Research Program through the National Research Foundation of Korea (NRF) funded by the Ministry of Science, ICT & Future Planning (NRF-2021R1A2C1006791) and the AI-based GIST Research Scientist Project grant funded by the GIST in 2024. KYK was also supported by the Creation of the Quantum Information Science R&D Ecosystem (Grant No. 2022M3H3A106307411) through the National Research Foundation of Korea (NRF) funded by the Korean government (Ministry of Science and ICT). All authors contributed equally to this paper and should be considered as co-first authors.

-
- [1] R. C. Hilborn, *Chaos and nonlinear dynamics: an introduction for scientists and engineers* (Oxford university press, 2000).
- [2] O. Bohigas, M. J. Giannoni, and C. Schmit, *Phys. Rev. Lett.* **52**, 1 (1984).
- [3] O. Bohigas, *Physical Review Letters* **52**, 1 (1984).
- [4] T. Guhr, A. Muller-Groeling, and H. A. Weidenmuller, *Phys. Rept.* **299**, 189 (1998), [arXiv:cond-mat/9707301](#).
- [5] O. Bohigas and M.-J. Giannoni, *Mathematical and Computational Methods in Nuclear Physics* (Springer Berlin Heidelberg, 31 May 2005).
- [6] M. V. Berry, *Proc. R. Soc. Lond.* **400**, 229 (1985).
- [7] S. Muller, S. Heusler, P. Braun, F. Haake, and A. Altland, *Phys. Rev. Lett.* **93**, 014103 (2004), [arXiv:nlin/0401021](#).
- [8] A. I. Larkin and Y. N. Ovchinnikov, *Sov Phys JETP* **28**, 1200 (1969).
- [9] G. P. Berman and G. M. Zaslavsky, *Physica A: Statistical Mechanics and its Applications* **91**, 450 (1978).
- [10] J. Maldacena, S. H. Shenker, and D. Stanford, *Journal of High Energy Physics* **2016** (2016), [10.1007/jhep08\(2016\)106](#).
- [11] S. H. Shenker and D. Stanford, *JHEP* **03**, 067 (2014), [arXiv:1306.0622 \[hep-th\]](#).
- [12] S. H. Shenker and D. Stanford, *JHEP* **05**, 132 (2015), [arXiv:1412.6087 \[hep-th\]](#).
- [13] A. M. García-García and J. J. M. Verbaarschot, *Phys. Rev. D* **94**, 126010 (2016).
- [14] J. S. Cotler, G. Gur-Ari, M. Hanada, J. Polchinski, P. Saad, S. H. Shenker, D. Stanford, A. Streicher, and M. Tezuka, *JHEP* **05**, 118 (2017), [Erratum: *JHEP* 09, 002 (2018)], [arXiv:1611.04650 \[hep-th\]](#).
- [15] J. de Boer, E. Lladrés, J. F. Pedraza, and D. Vegh, *Phys. Rev. Lett.* **120**, 201604 (2018), [arXiv:1709.01052 \[hep-th\]](#).
- [16] D. Stanford and E. Witten, *Adv. Theor. Math. Phys.* **24**, 1475 (2020), [arXiv:1907.03363 \[hep-th\]](#).
- [17] D. E. Parker, X. Cao, A. Avdoshkin, T. Scaffidi, and E. Altman, *Phys. Rev. X* **9**, 041017 (2019), [arXiv:1812.08657 \[cond-mat.stat-mech\]](#).
- [18] V. Balasubramanian, P. Caputa, J. M. Magan, and Q. Wu, *Phys. Rev. D* **106**, 046007 (2022), [arXiv:2202.06957 \[hep-th\]](#).
- [19] V. Balasubramanian, J. M. Magan, and Q. Wu, (2023), [arXiv:2312.03848 \[hep-th\]](#).
- [20] H. Tang, (2023), [arXiv:2312.17416 \[hep-th\]](#).
- [21] P. Caputa, H.-S. Jeong, S. Liu, J. F. Pedraza, and L.-C. Qu, *JHEP* **05**, 337 (2024), [arXiv:2402.09522 \[hep-th\]](#).
- [22] B. Bhattacharjee and P. Nandy, (2024), [arXiv:2407.07399 \[quant-ph\]](#).
- [23] K. Hashimoto, K. Murata, N. Tanahashi, and R. Watanabe, *JHEP* **11**, 040 (2023), [arXiv:2305.16669 \[hep-th\]](#).
- [24] H. A. Camargo, V. Jahnke, H.-S. Jeong, K.-Y. Kim, and M. Nishida, *Phys. Rev. D* **109**, 046017 (2024), [arXiv:2306.11632 \[hep-th\]](#).
- [25] V. Balasubramanian, R. N. Das, J. Erdmenger, and Z.-Y. Xian, (2024), [arXiv:2407.11114 \[hep-th\]](#).
- [26] E. Rabinovici, A. Sánchez-Garrido, R. Shir, and J. Sonner, *JHEP* **03**, 211 (2022), [arXiv:2112.12128 \[hep-th\]](#).
- [27] G. F. Scialchi, A. J. Roncaglia, and D. A. Wisniacki, *Phys. Rev. E* **109**, 054209 (2024), [arXiv:2309.13427 \[quant-ph\]](#).
- [28] A. Gill, K. Pal, K. Pal, and T. Sarkar, *Phys. Rev. B* **109**, 104303 (2024), [arXiv:2311.07892 \[quant-ph\]](#).
- [29] A. Bhattacharya, P. P. Nath, and H. Sahu, *Phys. Rev. D* **109**, 066010 (2024), [arXiv:2312.11677 \[quant-ph\]](#).
- [30] H. A. Camargo, K.-B. Huh, V. Jahnke, H.-S. Jeong, K.-Y. Kim, and M. Nishida, (2024), [arXiv:2405.11254 \[hep-th\]](#).
- [31] G. F. Scialchi, A. J. Roncaglia, C. Pineda, and D. A. Wisniacki, (2024), [arXiv:2407.06428 \[quant-ph\]](#).
- [32] E. Rabinovici, A. Sánchez-Garrido, R. Shir, and J. Sonner, *JHEP* **06**, 062 (2021), [arXiv:2009.01862 \[hep-th\]](#).
- [33] B. Bhattacharjee, P. Nandy, and T. Pathak, *JHEP* **08**, 099 (2023), [arXiv:2210.02474 \[hep-th\]](#).
- [34] N. Hörnedal, N. Carabba, A. S. Matsoukas-Roubeas, and A. del Campo, *Commun. Phys.* **5**, 207 (2022), [arXiv:2202.05006 \[quant-ph\]](#).

- [35] J. Erdmenger, S.-K. Jian, and Z.-Y. Xian, *JHEP* **08**, 176 (2023), [arXiv:2303.12151 \[hep-th\]](#).
- [36] S. Chapman, S. Demulder, D. A. Galante, S. U. Sheorey, and O. Shoval, (2024), [arXiv:2407.09604 \[hep-th\]](#).
- [37] P. Caputa and S. Liu, *Phys. Rev. B* **106**, 195125 (2022), [arXiv:2205.05688 \[hep-th\]](#).
- [38] M. Afrasiar, J. Kumar Basak, B. Dey, K. Pal, and K. Pal, (2022), [arXiv:2208.10520 \[hep-th\]](#).
- [39] P. Caputa, N. Gupta, S. S. Haque, S. Liu, J. Murugan, and H. J. R. Van Zyl, *JHEP* **01**, 120 (2023), [arXiv:2208.06311 \[hep-th\]](#).
- [40] K. Pal, K. Pal, A. Gill, and T. Sarkar, *Phys. Rev. B* **108**, 104311 (2023), [arXiv:2304.09636 \[quant-ph\]](#).
- [41] J. Kim, J. Murugan, J. Olle, and D. Rosa, *Phys. Rev. A* **105**, L010201 (2022), [arXiv:2109.05301 \[quant-ph\]](#).
- [42] A. Bhattacharyya, D. Ghosh, and P. Nandi, *JHEP* **12**, 112 (2023), [arXiv:2306.05542 \[hep-th\]](#).
- [43] B. Bhattacharjee, X. Cao, P. Nandy, and T. Pathak, *JHEP* **05**, 174 (2022), [arXiv:2203.03534 \[quant-ph\]](#).
- [44] K.-B. Huh, H.-S. Jeong, and J. F. Pedraza, *JHEP* **05**, 137 (2024), [arXiv:2312.12593 \[hep-th\]](#).
- [45] A. Bhattacharya, P. Nandy, P. P. Nath, and H. Sahu, *JHEP* **12**, 081 (2022), [arXiv:2207.05347 \[quant-ph\]](#).
- [46] B. Bhattacharjee, X. Cao, P. Nandy, and T. Pathak, *JHEP* **03**, 054 (2023), [arXiv:2212.06180 \[quant-ph\]](#).
- [47] V. Mohan, (2023), [arXiv:2308.10945 \[hep-th\]](#).
- [48] A. Bhattacharya, P. Nandy, P. P. Nath, and H. Sahu, *JHEP* **12**, 066 (2023), [arXiv:2303.04175 \[quant-ph\]](#).
- [49] B. Bhattacharjee, P. Nandy, and T. Pathak, *JHEP* **01**, 094 (2024), [arXiv:2311.00753 \[quant-ph\]](#).
- [50] E. Carolan, A. Kiely, S. Campbell, and S. Deffner, (2024), [arXiv:2404.03529 \[quant-ph\]](#).
- [51] P. Nandy, A. S. Matsoukas-Roubeas, P. Martínez-Azcona, A. Dymarsky, and A. del Campo, (2024), [arXiv:2405.09628 \[quant-ph\]](#).
- [52] X.-Y. Song, C.-M. Jian, and L. Balents, *Physical Review Letters* **119** (2017), [10.1103/physrevlett.119.216601](#).
- [53] A. Eberlein, V. Kasper, S. Sachdev, and J. Steinberg, *Physical Review B* **96** (2017), [10.1103/physrevb.96.205123](#).
- [54] A. M. García-García, B. Loureiro, A. Romero-Bermúdez, and M. Tezuka, *Phys. Rev. Lett.* **120**, 241603 (2018), [arXiv:1707.02197 \[hep-th\]](#).
- [55] T. Nosaka, D. Rosa, and J. Yoon, *Journal of High Energy Physics* **2018**, 41 (2018).
- [56] J. Kim and X. Cao, *Phys. Rev. Lett.* **126**, 109101 (2021), [arXiv:2004.05313 \[cond-mat.stat-mech\]](#).
- [57] A. M. García-García, B. Loureiro, A. Romero-Bermúdez, and M. Tezuka, *Phys. Rev. Lett.* **126**, 109102 (2021), [arXiv:2007.06121 \[cond-mat.str-el\]](#).
- [58] A. V. Lunkin, A. Y. Kitaev, and M. V. Feigel'man, *Phys. Rev. Lett.* **125**, 196602 (2020), [arXiv:2006.14535 \[cond-mat.str-el\]](#).
- [59] D. K. Nandy, T. Cadez, B. Dietz, A. Andreanov, and D. Rosa, *Phys. Rev. B* **106**, 245147 (2022), [arXiv:2206.08599 \[cond-mat.str-el\]](#).
- [60] H. G. Menzler and R. Jha, (2024), [arXiv:2403.14384 \[quant-ph\]](#).
- [61] D. Chowdhury, A. Georges, O. Parcollet, and S. Sachdev, *Rev. Mod. Phys.* **94**, 035004 (2022).
- [62] J. Kim and X. Cao, *Phys. Rev. Lett.* **126**, 109101 (2021).
- [63] F. Monteiro, T. Micklitz, M. Tezuka, and A. Altland, *Phys. Rev. Res.* **3**, 013023 (2021).
- [64] C. Lanczos, *J. Res. Natl. Bur. Stand. B* **45**, 255 (1950).
- [65] V. S. Viswanath and G. Müller, *The Recursion Method: Application to Many-Body Dynamics* (Springer Berlin, Heidelberg, Germany, 1994).
- [66] E. Brézin and S. Hikami, *Phys. Rev. E* **55**, 4067 (1997).
- [67] A. del Campo, J. Molina-Vilaplana, and J. Sonner, *Phys. Rev. D* **95**, 126008 (2017), [arXiv:1702.04350 \[hep-th\]](#).
- [68] E. Rabinovici, A. Sánchez-Garrido, R. Shir, and J. Sonner, *JHEP* **07**, 151 (2022), [arXiv:2207.07701 \[hep-th\]](#).
- [69] J. Erdmenger, S.-K. Jian, and Z.-Y. Xian, *Journal of High Energy Physics* **2023** (2023), [10.1007/jhep08\(2023\)176](#).
- [70] P. Amore, L. A. Pando Zayas, J. F. Pedraza, N. Quiroz, and C. A. Terrero-Escalante, (2024), [arXiv:2407.07259 \[hep-th\]](#).
- [71] J. Maldacena, *Journal of High Energy Physics* **2003**, 021 (2003).
- [72] E. Rabinovici, A. Sánchez-Garrido, R. Shir, and J. Sonner, *JHEP* **08**, 213 (2023), [arXiv:2305.04355 \[hep-th\]](#).
- [73] Y.-Z. You, A. W. W. Ludwig, and C. Xu, *Physical Review B* **95** (2017), [10.1103/physrevb.95.115150](#).
- [74] J. S. Cotler, G. Gur-Ari, M. Hanada, J. Polchinski, P. Saad, S. H. Shenker, D. Stanford, A. Streicher, and M. Tezuka, *Journal of High Energy Physics* **2017** (2017), [10.1007/jhep05\(2017\)118](#).
- [75] C. Krishnan, K. V. Pavan Kumar, and D. Rosa, *Journal of High Energy Physics* **2018** (2018), [10.1007/jhep01\(2018\)064](#).
- [76] B. N. Parlett, *The Symmetric Eigenvalue Problem* (Society for Industrial and Applied Mathematics, 1998).

SUPPLEMENTAL MATERIAL

In this Supplementary Material, we offer additional details on the numerical computations discussed in the main text and present further analyses to corroborate our findings.

I. BLOCK DIAGONALIZATION OF THE SYK HAMILTONIAN

Block diagonalization of the Hamiltonian matrix is crucial for analyzing spectral statistics of the energy spectrum. By decomposing the Hamiltonian into smaller blocks based on the system's symmetries, the statistical properties of the energy levels can be studied more efficiently. This approach simplifies computations, improves numerical accuracy, and reduces the effective size of the system.

Regarding the SYK model, its Hamiltonian possesses a conserved charge parity operator P [73–75],

$$P = \begin{cases} (-i\chi_1\chi_2)(-i\chi_3\chi_4)\cdots(-i\chi_{N-1}\chi_N) & N \in \text{even}, \\ (-i\chi_1\chi_2)(-i\chi_3\chi_4)\cdots(-i\chi_N\chi_\infty) & N \in \text{odd}, \end{cases} \quad (10)$$

where χ_i ($i = 1, 2, \dots, N$) are Majorana fermions, and N is the system size. The SYK Hamiltonian H commutes with the parity operator P , $[H, P] = 0$, allowing the Hamiltonian to be block diagonalized. Using an invertible matrix consisting of the eigenvectors of P , the system is split into parity-even and parity-odd sectors, each with a dimension $d = 2^{\frac{N}{2}-1}$. Fig. 4 illustrates the typical block diagonalized Hamiltonian of a mass-deformed SYK model at finite κ .

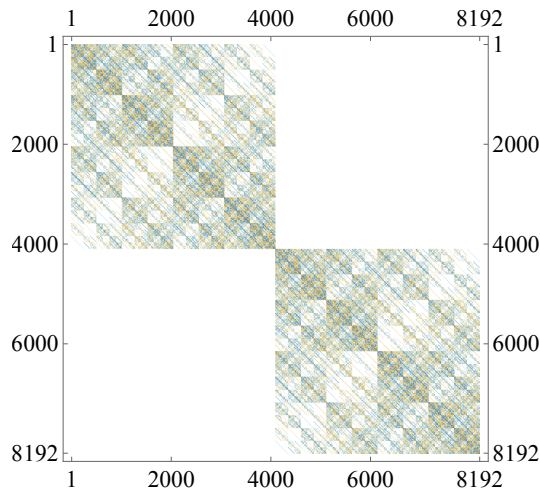


Figure 4. The block diagonalized mass-deformed SYK model for $N = 26$ and $\kappa = 1$. The top-left block corresponds to the parity-odd sector, while the bottom-right block corresponds to the parity-even sector.

In our study, we have focused on numerical computations within the parity-even sector for $N = 26$, using both WOLFRAM MATHEMATICA and MATLAB to cross-verify our results. We have also confirmed that the parity-odd sector produces similar outcomes for Krylov complexity.

II. LANZOS COEFFICIENTS AND QUANTUM CHAOS

In the main text, we focused on the Krylov complexity derived from solving the Schrödinger equation using the given Lanczos coefficients $\{a_n, b_n\}$. Here, we examine the Lanczos coefficients $\{a_n, b_n\}$ of the mass-deformed SYK models. As suggested in references [23, 76], the Lanczos coefficients can be obtained through the Lanczos algorithm, which minimizes numerical errors in the orthogonalization process, ensuring consistency with those derived from the Hessenberg form. The algorithm is outlined as follows:

1. Initialize with $b_0 := 0$, $|K_0\rangle := |\psi(0)\rangle$, $a_0 := \langle K_0|\mathcal{D}|K_0\rangle$, where $\mathcal{D} := \text{diag}(E_1, \dots, E_d)$.
2. For $n \geq 1$: Compute $|A_n\rangle = (\mathcal{D} - a_{n-1})|K_{n-1}\rangle - b_{n-1}|K_{n-2}\rangle$.
3. Replace $|A_n\rangle \rightarrow |A_n\rangle - \sum_{m=0}^{n-1} \langle A_m|K_0\rangle |A_m\rangle$.

4. Set $b_n = \langle A_n | A_n \rangle^{1/2}$.

5. If $b_n = 0$, terminate the algorithm; otherwise, set $|K_n\rangle = b_n^{-1} |A_n\rangle$ and $a_n = \langle K_n | \mathcal{D} | K_n \rangle$, then return to step 2.

In our study, we utilize the TFD state as the initial state $|\psi(0)\rangle$. To illustrate our numerical results, we present specific computations for the maximally entangled state, i.e., the TFD state with $\beta = 0$. Using the Lanczos algorithm, we obtain the Lanczos coefficients for the mass-deformed SYK model, as shown in Fig. 5 below. We observe that a_n exhibits oscillatory behavior, while b_n initially grows (see inset), reaches a peak, and then diminishes as n approaches the dimension of the Krylov space ($\kappa = 0$) [18] and in RMT [35].

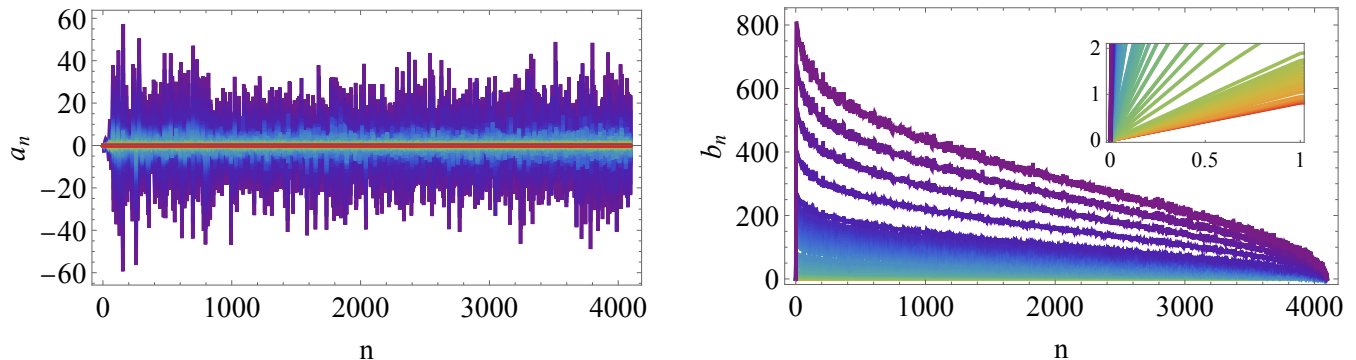


Figure 5. Lanczos coefficients $\{a_n, b_n\}$ for the mass-deformed SYK model for various values of the mass-deformation parameter, ranging from $\kappa = 0$ (red) to $\kappa = 300$ (purple).

Two notable observations regarding the effect of κ are as follows. First, as κ increases, the slope of the initial growth of b_n also increases (see the inset), indicating that the value of b_1 is enhanced by the mass deformation parameter. This enhancement may explain the behavior of the slope of $C(t)$ in Fig. 1 with increasing κ , as the early-time behavior of the Krylov complexity has been shown to follow $C(t \ll 1) \approx b_1^2 t^2$ [44]. The second observation concerns the variance of the Lanczos coefficients, defined as [23]

$$\begin{aligned} \sigma_a^2 &:= \text{Var}(x_i^{(a)}), & x_i^{(a)} &:= \log\left(\frac{a_{2i-1}}{a_{2i}}\right), \\ \sigma_b^2 &:= \text{Var}(x_i^{(b)}), & x_i^{(b)} &:= \log\left(\frac{b_{2i-1}}{b_{2i}}\right). \end{aligned} \quad (11)$$

For additional information on the variance of Lanczos coefficients in the context of Krylov operator complexity, see [26, 68]. We observe that the variance increases in the integrable regime (large κ) compared to the chaotic regime (small κ). This trend is especially pronounced for σ_b^2 ; see Fig. 6. However, unlike the KCP, we do not observe a distinct feature indicative of a critical phase transition around $\kappa_c \approx 66$. This suggests that the KCP may serve as a more effective order parameter than the Lanczos coefficients themselves. Refer to Fig. 7 for the histogram plot of the Lanczos coefficients' distribution, which supports the conclusions drawn from the variance analysis.

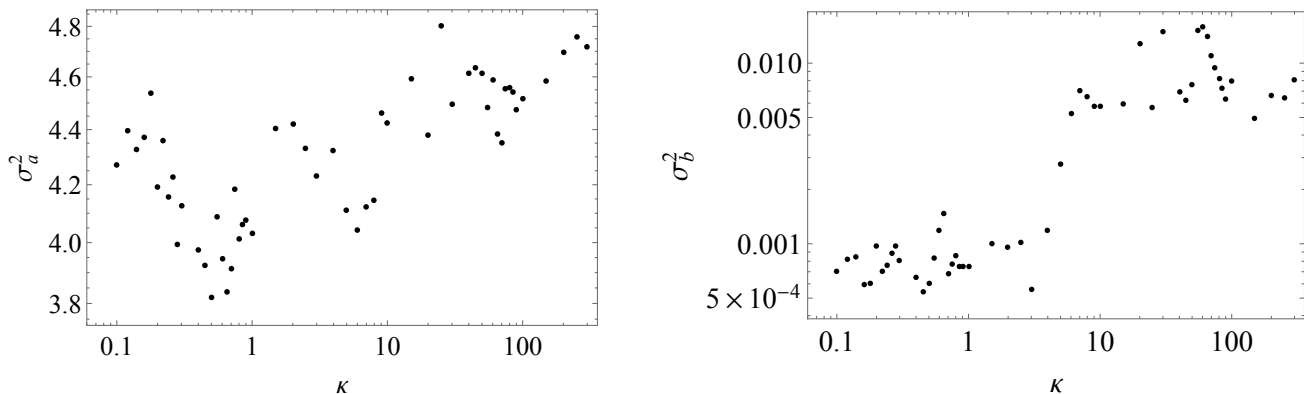


Figure 6. The variance of the Lanczos coefficients $\sigma_{a,b}^2$ as a function of κ .

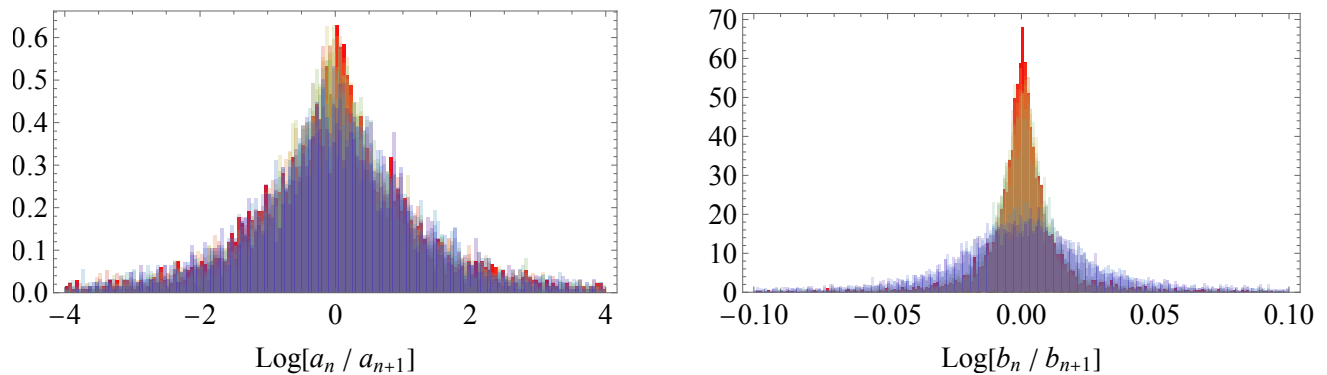


Figure 7. Histogram of the Lanczos coefficients a_n (left panel) and b_n (right panel) for values of κ ranging from $\kappa = 0$ (red) to $\kappa = 300$ (purple).

III. NORMALIZATION CONDITION AND EHRENFEST THEOREM

We have confirmed that our numerical results meet essential consistency checks, including the wave function normalization condition [18] and the Ehrenfest theorem [69].

First, we address the normalization condition for the Krylov wave functions,

$$\sum_n |\psi_n(t)|^2 = 1, \quad (12)$$

which ensures the unitarity of time evolution. As shown in Fig. 8, this normalization condition is satisfied within our time window for numerical computations of Krylov complexity, specifically for $t \leq 2^{N/2+1}$. To maintain normalization over a longer time window, including the late-time regime, it is necessary to consider larger values of n_{\max} , as discussed in [23, 24]. Our results indicate that the chosen cutoff value of $n_{\max} = d$ is adequate for capturing all key features of Krylov complexity—the initial ramp, peak, decline, and plateau—while satisfying the normalization condition.

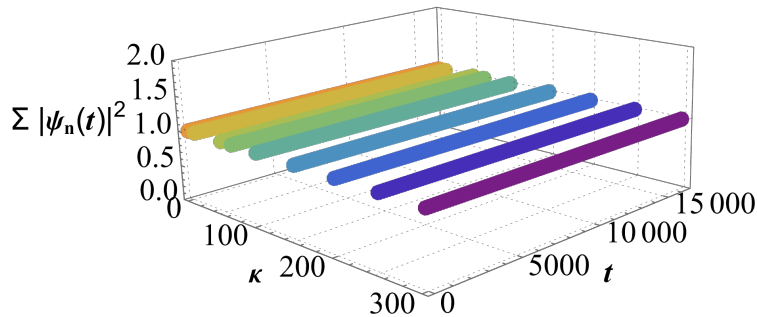


Figure 8. The normalization condition of the Krylov wave functions.

Second, an important aspect of Krylov complexity is its adherence to the Ehrenfest theorem [35], expressed as:

$$\partial_t^2 C(t) = -[[C(t), \mathcal{L}], \mathcal{L}], \quad (13)$$

where $\mathcal{L} = H \otimes \mathbb{I}$ denotes the Liouvillian and \mathbb{I} represents the identity operator. By applying the Schrödinger equation along with the definition of Krylov complexity, the Ehrenfest theorem (13) can be formulated in terms of the Lanczos coefficients and the Krylov wave functions as follows:

$$\partial_t^2 C(t) = 2 \sum_n [(b_{n+1}^2 - b_n^2) \psi_n(t) \psi_n^*(t) + (a_{n+1} - a_n) b_{n+1} \psi_{(n+1)}(t) \psi_n^*(t)], \quad (14)$$

where $\mathcal{T}_a \tilde{\mathcal{T}}_b := \frac{1}{2} (\mathcal{T}_a \tilde{\mathcal{T}}_b + \mathcal{T}_b \tilde{\mathcal{T}}_a)$. In Fig. 9, we validate the Ehrenfest theorem for mass-deformed SYK models, demonstrating the relationship between the second time derivative of Krylov complexity and a combination of Lanczos coefficients. It is important to emphasize that this relationship, as expressed in (14), holds universally for any system by construction. This verification strengthens the reliability of our numerical results.

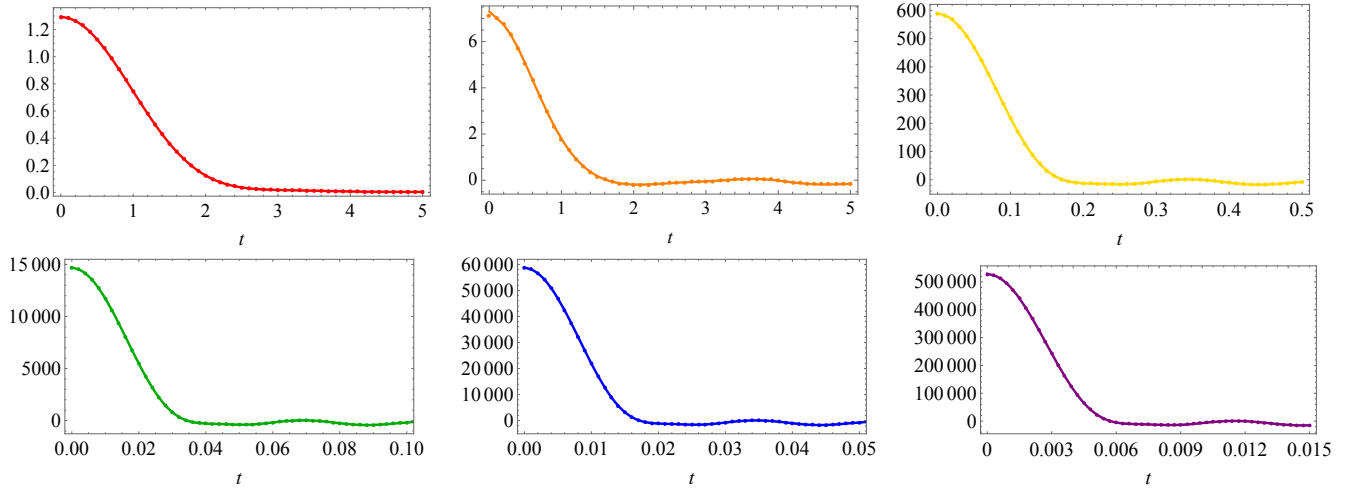


Figure 9. Ehrenfest theorem in the mass-deformed SYK models for $\kappa = 0, 1, 10, 50, 100, 300$ (red, orange, yellow, green, blue and purple, respectively). The solid lines correspond to the L.H.S. of (14), while the dots represent the R.H.S. of (14).